SUPPLEMENTARY APPENDIX

Targeting the Ataxia Telangiectasia Mutated-null phenotype in chronic lymphocytic leukemia with pro-oxidants

Angelo Agathanggelou,[1] Victoria J. Weston,[1] Tracey Perry,[1] Nicholas J. Davies,[1] Anna Skowronska,[1] Daniel T. Payne,[2] John S. Fossey,[2] Ceri E. Oldreive,[1] Wenbin Wei,[1] Guy Pratt,[1,3] Helen Parry,[3] David Oscier,[4] Steve J. Coles,[5] Paul S. Hole,[5] Richard L. Darley,[5] Michael McMahon,[6] John D. Hayes,[6] Paul Moss,[1] Grant S. Stewart,[1] A. Malcolm R. Taylor,[1] and Tatjana Stankovic[1]

[1]School of Cancer Sciences, University of Birmingham; [2]School of Chemistry, University of Birmingham; [3]Haematology Department, Birmingham Heartlands Hospital; [4]Haematology Department, Royal Bournemouth Hospital, Dorset; [5]Department of Haematology, Institute of Cancer and Genetics, Cardiff University School of Medicine, Cardiff; [6]Medical Research Institute, University of Dundee, UK

 doi:10.3324/haematol.2014.115170
AA and VJW contributed equally to this work. The online version of this article has a Supplementary Appendix.
Manuscript received on October 20, 2014. Manuscript accepted on March 25, 2015.
Correspondence: t.stankovic@bham.ac.uk

Supplementary Table S1. Characteristics of CLL samples

CLL samples were stratified based on *ATM* mutation, *TP53* mutation and 11q deletion status and phosphorylation of the ATM targets ATM, SMC1, p53 and KAP1 in response to 5Gy IR. CLL samples were considered to be *ATM* wild type (ATM-wt) if no mutation changes were detected by Sanger sequencing and if they exhibited a normal ATM-dependent response to IR. Samples were considered to be *ATM* mutant if they were found to harbour at least one mutant *ATM* allele and exhibit impaired ATM-dependent responses to DNA damage. Most *ATM* mutant tumours had evidence of biallelic *ATM* inactivation (caused by 11q deletion and an *ATM* mutation), apart from CLL69, where a single mutation rendered the ATM response to be defective.

CLL sample	TP53 mutation status	ATM mutation status	11q deletion	Biallelic or monoallelic ATM inactivation	ATM dependent DNA damage response
CLL69	WT	6815delA	A	M	D
CLL124	WT	5228C/T	P	B	D
CLLRW	WT	2282delCT, 7890delA	A	B	D
CLL57	WT	2308G/T	P	B	D
CLLJF	WT	del49 TTCT	A	NK	D
CLL152	WT	8839A/T	P	B	D
CLL166	WT	8977C/T	P	B	D
CLL15	WT	7047C/G	P	B	D
CLL77	WT	1058del2, 5224G/C	A	B	D
CLL96	WT	5041A/G,5044G/T, ins9(exon 22)	A	B	D
CLLCW	WT	WT	A	A	NK
CLLHR	WT	WT	A	A	N
CLL158	WT	WT	A	A	N
CLLRR	WT	WT	A	A	N
CLLJW	WT	WT	A	A	N
CLL17	WT	WT	A	A	N
CLL133	WT	WT	A	A	N
CLL23	WT	WT	A	A	N
CLLLP	WT	WT	A	A	NK
CLLJB	WT	WT	A	A	N
CLLVM	WT	WT	A	A	N
CLLAC	WT	WT	A	A	N
CLLMM	WT	WT	P	M	NK
CLLBK	WT	WT	P	M	NK
CLL172	WT	WT	P	M	NK
CLL48	658del2, 849insC	WT	A	A	NK
CLL120	752T/G, 830del21	WT	A	A	N
CLL117	711G/A	WT	A	A	N

Key: P=present; A=absent; NK=not known; WT= wild type; M=monoallelic; B=biallelic; D=defective; N=normal

Supplementary Table S2. Comparison of PTL yield from different plant source extractions

Entry	Plant type	Fresh plant matter (kg)	Crude extract (g)	Parthenolide (g)	w/w % content
1	Feverfew source 1 (*Tanacetum parthenium)*[a]	4.57	19.259	1.319	0.029
2	Golden Dwarf Feverfew (*Tanacetum parthenium aureum)*[a]	0.076	0.213	0.061	0.080
3	Feverfew source 2 (*Tanacetum parthenium)*[b]	1.91	7.740	1.076	0.056
4	Feverfew source 3 (*Tanacetum parthenium)*[c]	5.27	21.270	1.846	0.035
5	Tansy (*Tanacetum vulgare)*[a]	5.70	14.491	4.865	0.085

[a]Seeds purchased from *CN Seeds* and grown under glass at Winterbourne Botanic Garden (Birmingham, UK)

[b]Seed heads collect from plants in the Birmingham local area and grown under glass at Winterbourne Botanic Garden (Birmingham, UK)

[c]Self sown plants collect from the grounds of Winterbourne Botanic Garden (Birmingham, UK) and maintained under glass.

Supplementary Table S3. Primer sequences for Q-PCR

Gene	Forward	Reverse
NRF2	CGGTATGCAACAGGACATTG	GTTTGGCTTCTGGACTTGGA
NQO1	GCCGCAGACCTTGTGATATT	TGAACACTCGCTCAAACCAG
GCLM	CCAGATGTCTTGGAATGCAC	CCATGTCAACTGCACTTCT
GSR	ACTTGCCCATCGACTTTTTG	CATCTTCCGTGAGTCCCACT
HMOX1	CCAGGCAGAGAATGCTGAGT	CTTGTTGCGCTCAATCTCCT
β-ACTIN	CACCATTGGCAATGAGCGGTTC	AGGTCTTTGCGGATGTCCACGT

Supplementary Table S4. SiRNAs sequences for transient transfection.

Gene	Forward	Reverse
ATM	Stealth siRNA (Life Technologies)	Stealth siRNA (Life Technologies)
KEAP1	GGCCUUUUGGCAUCAUGAAC[dT][dT]	GUUCAUGAUGCCAAAGGCC[dT][dT]
BRCA1-1	GCUCCUCUCACUCUUCAGU[dT][dT]	ACUGAAGAGUGAGAGGAGC[dT][dT]
BRCA1-2	AAGCUCCUCUCACUCUUCAGC[dT][dT]	ACUGAAGAGUGAGAGGAGCUU[dT][dT]
Scrambled	UGUGCACGUGCCGCUCGUC[dT][dT]	GACGAGCGGCACGUGCACA[dT][dT]

Supplementary materials and methods

Extraction and derivatisation of parthenolide

General Information

Commercially available solvents and reagents were used without further purification. ^{1}H NMR spectra were recorded at 400 MHz on a Bruker AVIII400 NMR spectrometer at room temperature. ^{13}C NMR spectra were recorded at 101 MHz on a Bruker AVIII400 NMR spectrometer at room temperature and are proton decoupled. All 2D NMR spectra were recorded on a Bruker AVIII400 NMR spectrometer at room temperature. Data was processed on Mestrec version 6.0.2-5475 and Topspin 2.0 (version of Nov 9th 2006). Chemical shifts (δ) are reported in ppm relative to residual NMR solvent peaks for ^{1}H NMR and ^{13}C NMR, coupling constants (*J*) are expressed in Hertz (Hz). Mass spectra were recorded with an electrospray MS Waters LCT time of flight Mass spectrometer or with an EI (GC/MS) Waters GCT Premier Time of Flight Mass Spectrometer. Infrared spectra were recorded on a PerkinElmer 100FT-IR spectrometer at room temperature.

Extraction

(3a*S*,9a*R*,10a*R*,10b*S*,*E*)-6,9a-Dimethyl-3-methylene-3a,4,5,8,9,9a,10a,10b-octahydrooxireno[2',3':9,10]cyclodeca[1,2-b]furan-2(3H)-one (PTL)

Fresh plant matter (detailed in Supplementary Table S2) was chopped into small pieces and manually stirred in water (80 ˚C, 200 gL^{-1}) for 10 minutes. The resulting solution was filtered and the filtrate extracted with chloroform (2:1 aqueous:organic). The organic phases were combined, dried over $MgSO_4$and reduced *in vacuo* to afford a brown viscous oil. This was purified by column chromatography on a CombiFlash R_F 200i with a 330g silica column cartridge, ELSD detection using an ethyl acetate/hexane gradient method to afford crude parthenolide as a yellow solid. Recrystallisation from hexane/ethyl acetate afforded parthenolide as a colourless crystalline solid. Absolute stereochemistry was confirmed by X-ray crystallography. Crystal data: $C_{15}H_{20}O_3$, *M*= 248.31, orthorhombic, *a*= 11.80140(10), *b*= 11.97233(9), *c*= 18.82978(13) Å, *U*= 2660.46(3) Å^3, *T*= 99.99(10) K, space group $P2_12_12_1$, *Z*= 8 and *Z'*= 2, 25179 reflections measured, 5341 unique (*R*int= 0.0225) which were used in all calculations. The final *R*1 was 0.0268 ($I>2\sigma(I)$) and w*R*(F2) was 0.0693 (all data). Flack parameter = 0.01(4). This structure is a polymorph of an X-ray crystal structure determined at room temperature with *Z'*= 1 published on three previous occasions; CSD ref codes: ARTINB, ARTINB01 and ARTINB02.[1] CCDC-1012153 contains the supplementary crystallographic data for this structure. These data can be obtained free of charge from The Cambridge Crystallographic Data Centre *via* http://www.ccdc.cam.ac.uk/Community/Requestastructure/pages/DataRequest.aspx.

^{1}H NMR (400 MHz, $CDCl_3$): δ (ppm) 6.33 (d, *J* = 3.7, 1H), 5.63 (d, *J* = 3.3, 1H), 5.21 (dd, *J* = 12.1, 2.5, 1H), 3.86 (t, *J* = 8.6, 1H), 2.85 – 2.72 (m, 2H), 2.51 – 2.32 (m, 2H), 2.24 – 2.07 (m, 4H), 1.79 – 1.68 (m, 4H), 1.33 – 1.20 (m, 4H).; ^{13}C NMR (101 MHz, $CDCl_3$): δ (ppm) 169.3, 139.3, 134.6, 125.3, 121.2, 82.5, 66.4, 61.5, 47.7, 41.2, 36.4, 30.7, 24.2, 17.3, 17.0.; FT-IR (ATR): v (cm^{-1}) 1656.46, 1752.65, 2862.90, 2933.53, 2980.48.;MS (TOF ES+): (m/z) 249.1 $[M+H]^+$, 271.1 $[M+Na]^+$, 287.1 $[M+K]^+$.; HRMS (m/z): $[M]^+$ Calcd for $C_{15}H_{20}NaO_3$, 271.1310; found, 271.1311.; mp: 114-116 °C (Supplementary Figures S1A and S1B).

Synthesis

(3*R*,3a*S*,9a*R*,10a*R*,10b*S*,*E*)-3-((Dimethylamino)methyl)-6,9a-dimethyl-3a,4,5,8,9,9a,10a,10b-octahydrooxireno[2',3':9,10]cyclodeca[1,2-b]furan-2(3H)-one (DMAPT) Dimethylamine (2M in MeOH, 1.2 mL, 2.4 mmol, 1.5 equiv.) was added to a stirred solution of parthenolide (400 mg, 1.6 mmol, 1 equiv.) in MeOH (14 mL) for 21 hours at room temperature (Supplementary Figure S2A). The reaction mixture was reduced *in vacuo* to afford the desired compound with no further purification needed as a white solid (0.35 g, 74%). ^{1}H NMR (400 MHz, $CDCl_3$): δ (ppm) 5.21 (dd, *J* = 11.9, 2.2, 1H), 3.83 (t, *J* = 9.0, 1H), 2.78 – 2.70 (m, 2H), 2.63 (dd, *J* = 13.2, 4.8,1H), 2.47 – 2.32 (m, 2H), 2.28 – 2.01 (m, 12H), 1.70 (s, 2H), 1.69 – 1.59 (m, 1H), 1.30 (s, 3H), 1.22 (td, *J* = 13.0, 5.9, 1H).; ^{13}C NMR (101 MHz, $CDCl_3$): δ (ppm) 176.5, 134.7, 125.0, 82.1, 66.5, 61.5, 57.7, 47.9, 46.5, 46.2, 41.1, 36.7, 29.9, 24.1, 17.2, 16.9.; FT-IR (ATR): ν (cm^{-1}) 1754, 2765, 2806, 2826, 2860, 2926.; MS (TOF ES+): (m/z) 294.2 $[M+H]^+$.; HRMS (m/z): $[M]^+$ Calcd for $C_{17}H_{28}NO_3$, 294.2069; found, 294.2064.; mp: 145-147 °C (Supplementary Figure S2B and S2C).

1-((3*R*,3a*S*,9a*R*,10a*R*,10b*S*,*E*)-6,9a-Dimethyl-2-oxo-2,3,3a,4,5,8,9,9a,10a,10b-decahydrooxireno[2',3':9,10]cyclodeca[1,2-b]furan-3-yl)-*N*,*N*-dimethylmethanaminium chloride (DMAPT-HCl) Hydrochloric acid gas was passed over a stirred solution of dimethylamineparthenolide (248 mg, 0.85 mmol) in Et_2O (50 mL) until a white precipitate formed (< 5min) (Supplementary Figure S1). The reaction mixture was reduced *in vacuo* to afford the desired compound as a white solid (0.28 g, >99%, 10:1 HCl salt:free amine by 1H NMR spectroscopy in D_4-MeOH). ^{1}H NMR (400 MHz, d_4-MeOH): δ (ppm) 5.29 (app d, *J* = 10.7, 1H), 4.17 (t, *J* = 9.1, 1H), 3.55 – 3.25 (m, 2H (minus overlapping residual MeOH CH_3)), 3.13 – 3.01 (m, 1H), 3.00 – 2.76 (m, 7H), 2.49 (ddd, *J* = 17.9, 13.3, 5.3 Hz, 1H), 2.36 – 1.70 (m, 10H), 1.41 – 1.10 (m, 5H).; ^{13}C NMR (101 MHz, d_4-MeOH): δ (ppm) 176.49, 134.46, 124.80, 83.10, 65.95, 61.91, 56.14, 47.51, 43.52, 43.15, 40.38, 36.18, 28.69, 23.58, 16.10, 15.63.; FT-IR (ATR): ν (cm^{-1}) 1755, 2765, 2826, 2861, 2926, 3373 (broad).; MS (TOF ES+): (m/z) 294.2 $[M+H]^+$.; HRMS (m/z): $[M]^+$ Calcd for $C_{17}H_{28}NO_3$, 294.2069; found, 294.2066.; mp: 110-112 °C (Supplementary Figures S3A and S3B).

Cross-linking Chromatin Immunoprecipitation (XChIP)

XChIP was applied to 10-20x10^6 primary CLL cells with and without treatment with 100μM tBHQ for 6 hours. Following treatment, cells were harvested, washed three times in PBS/1μM PMSF (Sigma) and fixed in 2mM disuccinimidyl glutarate (Sigma). Cells were then fixed in 1% formaldehyde (Sigma) and cross-linking was terminated by incubation in 0.116M glycine (Sigma). To generate lysates for immunoprecipitation samples were incubated sequentially in Cell Lysis Buffer (5mM PIPES pH 8 (Sigma), 85mM KCl (Sigma), 0.5% NP40 (Sigma), 1μM PMSF, Protease inhibitor cocktail (Roche)) and RIPA Buffer (150mM NaCl (Sigma), 1% NP40, 0.5% NaDoc (Sigma), 0.1% SDS (Sigma), 50mM TrisHCl pH 8 (Sigma), 1μM PMSF, Protease inhibitor cocktail for 10 minutes followed by sonication in a Sonomatic waterbath (Model S0375) for 1 hour. Lysates were pre-cleared with Protein A sepharose beads (Sigma) and incubated overnight with 5μg of antibody or pre-immune serum. Antibody-protein/DNA complexes were immobilised on Protein A sepharose beads and DNA was recovered by incubation in Proteinase K (Ambion) followed by extraction in phenol/chloroform/isoamyl-alcohol. SYBR-green Real-Time PCR was used to quantify immunoprecipitated DNA. Data was expressed as percentage of input DNA using the comparative Ct method.

Mitochondrial ROS Assay

Mitochondrial superoxide was measured using MitoSox Red (Invitrogen) and flow cytometry in accordance with the manufacturer's instructions. Apoptotic cells were eliminated from analysis by labelling with Annexin V-APC (Invitrogen). MitoSox Red in non-apoptotic cells was quantified using a BD Biosciences LSR II flow cytometer with BD FACSDiva software. For positive and negative controls, cells were pretreated with 50μg/ml Antimycin A (Sigma) or 5μM iron (III) 5, 10, 15, 20-tetrakis-4-carboxyphenyl porphyrin (FeTCPP; Frontier Scientific Inc), respectively.

Immunoblotting

Antibodies used for immunoblotting: mouse anti-ATM , rabbit anti–phospho-ATM (Rockland Immunochemicals, PA, USA), rabbit anti-SMC1, rabbit anti-phospho SMC, rabbit anti-KAP1, rabbit anti-phospho KAP1 (Bethyl Laboratories, TX, USA), rabbit anti-phospho p53, rabbit anti-PARP (Cell Signaling, MA 01923, USA), rabbit anti-NRF2 (C20, H300), goat anti-KEAP1, rabbit anti-MafF/G/K, goat anti-BACH1, goat anti-LAM B and rabbit anti-AIF (Santa Cruz Biotechnology, Germany), rabbit anti-TUBB1 and mouse anti-β-ACTIN (Sigma-Aldrich).

Reference

1. D.G.Leppard, M.Rey, A.S.Dreiding and R.Grieb, *Helv. Chim. Acta*, 1974, **57**, 602: M.R.Uskokovic, T.H.Williams and J.F.Blount, *Helv. Chim. Acta*, 1974, **57**, 600: I.M.Yusupova, B.Tashkhodzhaev and A.Mallabaev, *Khim.Prir.Soedin*, 1986, 788.

Supplementary Figure S1. (A) ^{1}H NMR spectrum of PTL (d_4-MeOH) and (B) ^{13}C NMR spectrum of PTL (d_4-MeOH).

A

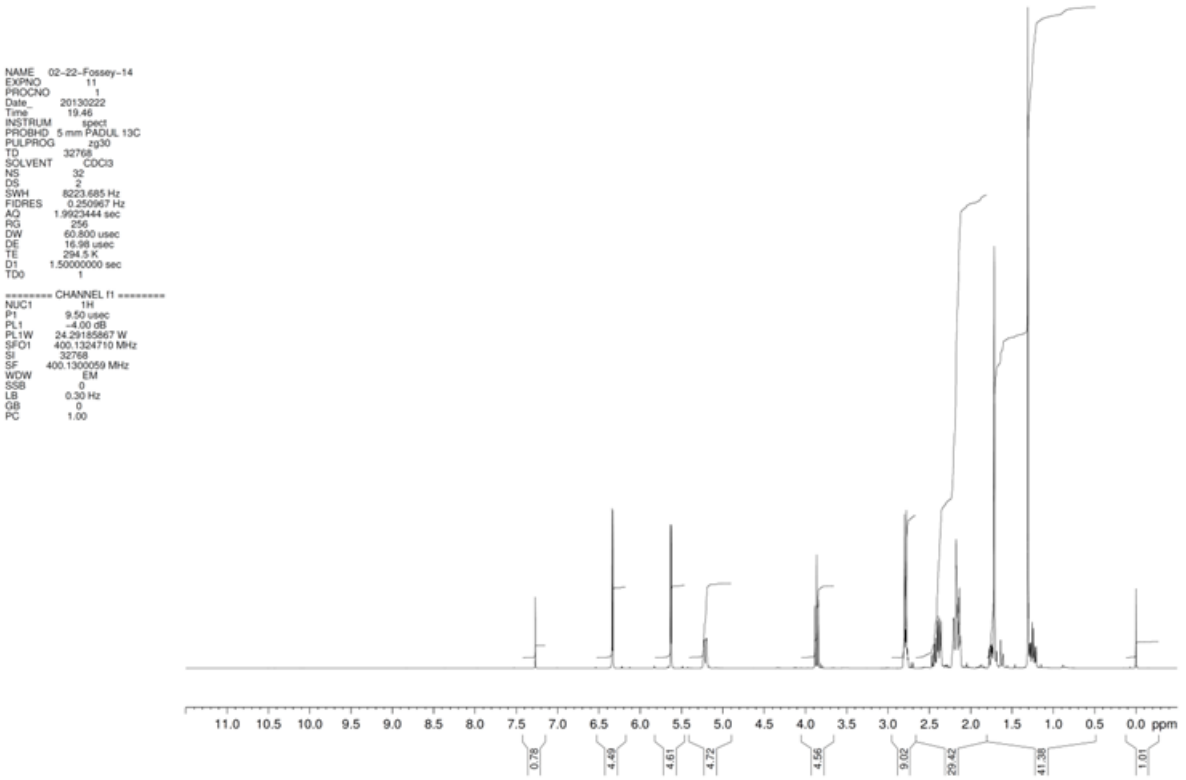

B

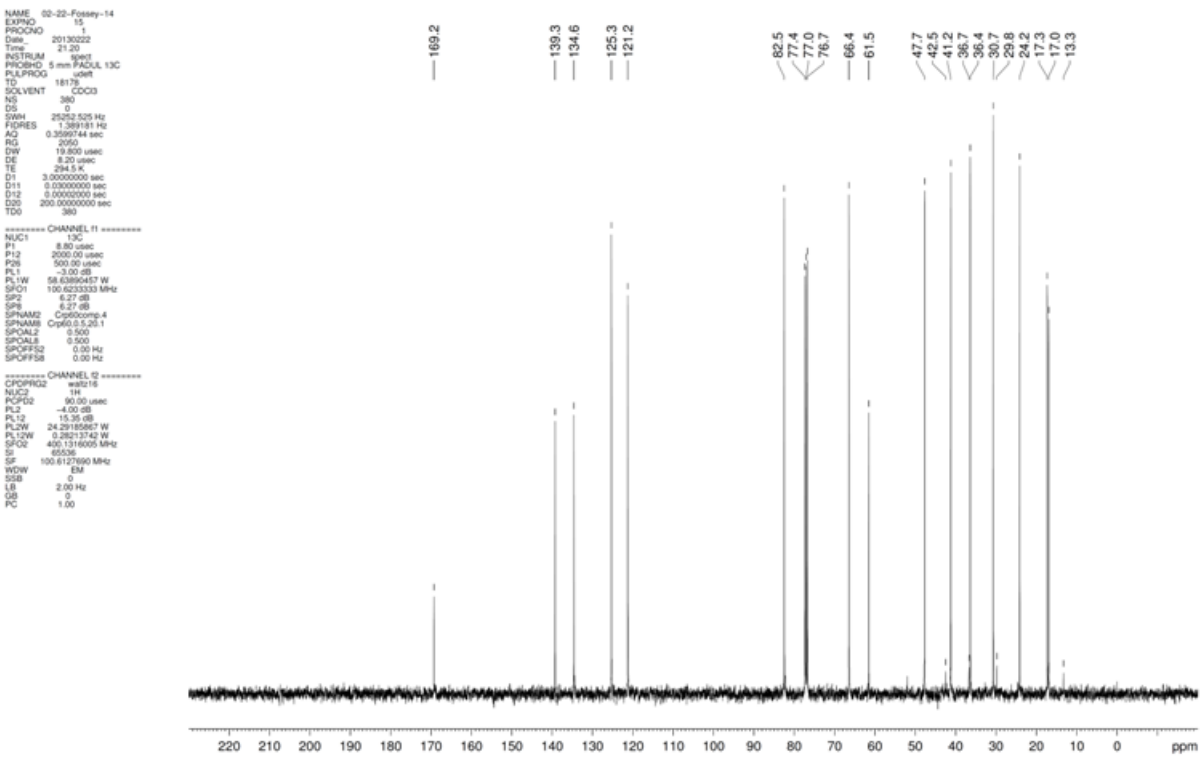

Supplementary Figure S2. (A) Schematic summarising the synthesis of DMAPT-HCl from PTL. (B) ^{1}H NMR spectrum of DMAPT (d_4-MeOH) and (C) ^{13}C NMR spectrum of DMAPT (d_4-MeOH)

A

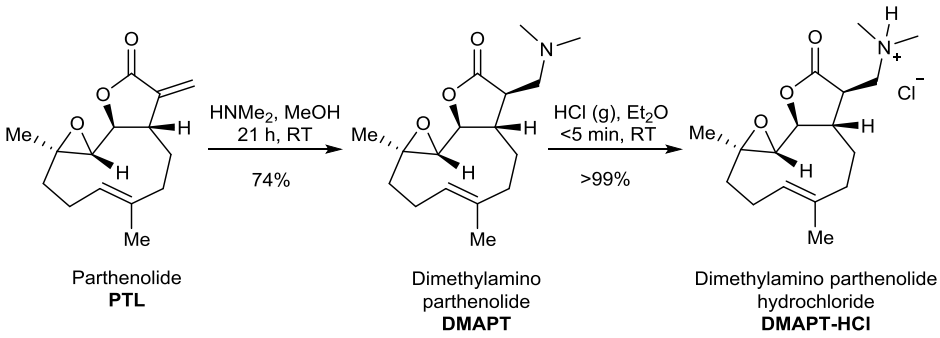

Parthenolide
PTL

Dimethylamino parthenolide
DMAPT

Dimethylamino parthenolide hydrochloride
DMAPT-HCl

B

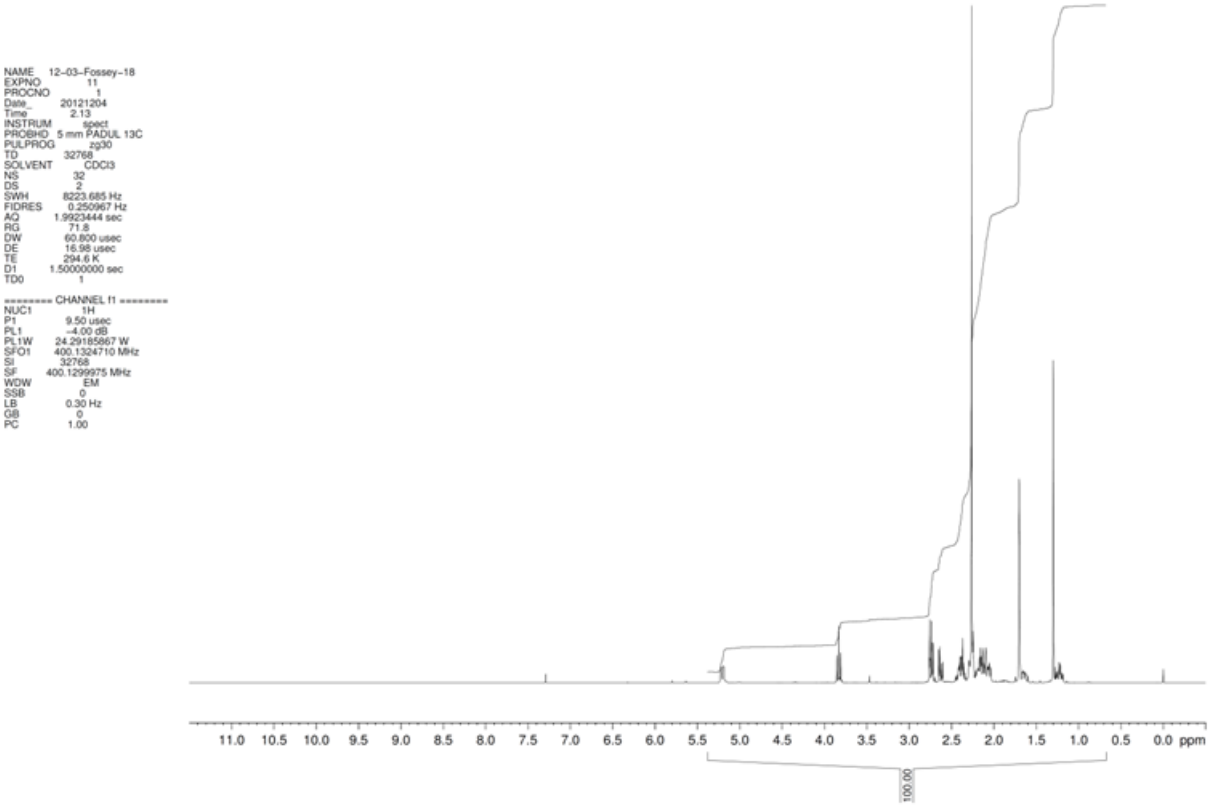

C

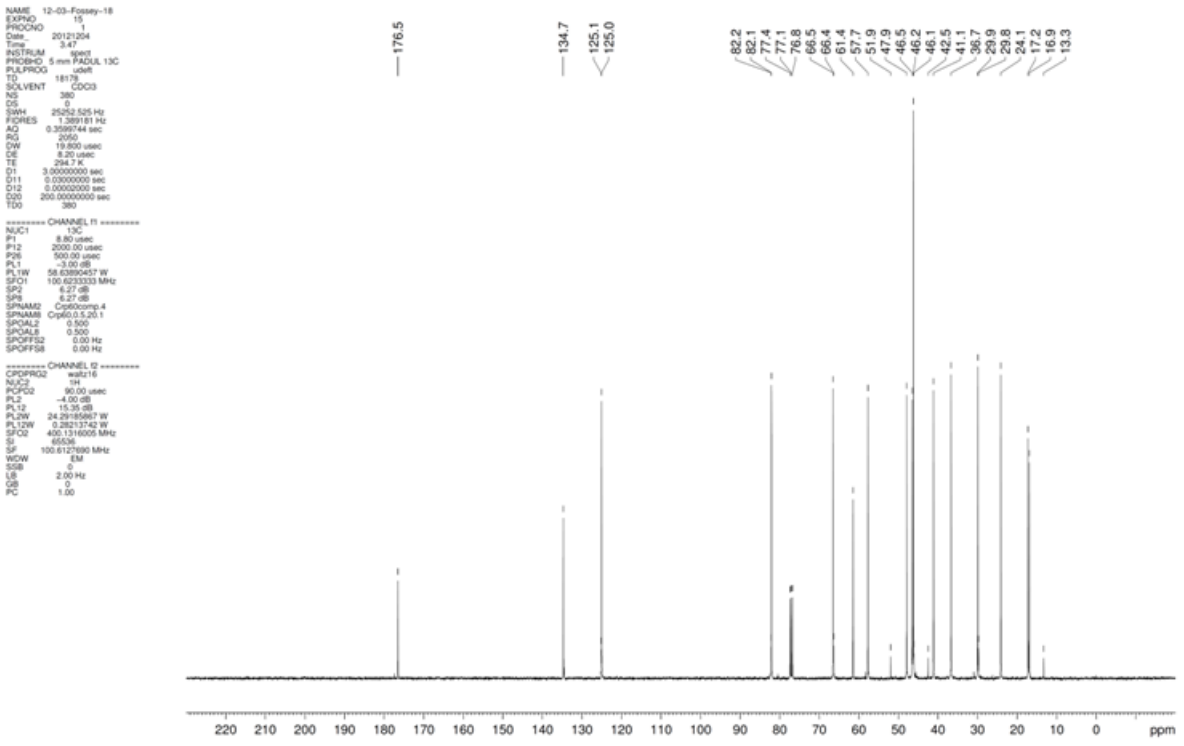
NAME 12--03--Fossey--18
EXPNO 15
PROCNO 1
Date_ 20121204
Time 3.47
INSTRUM spect
PROBHD 5 mm PADUL 13C
PULPROG udeft
TD 18176
SOLVENT CDCl3
NS 380
DS 0
SWH 25252.525 Hz
FIDRES 1.389181 Hz
AQ 0.3599744 sec
RG 2050
DW 19.800 usec
DE 8.20 usec
TE 294.7 K
D1 3.00000000 sec
D11 0.03000000 sec
D12 0.00002000 sec
D20 200.00000000 sec
TD0 380
======== CHANNEL f1 ========
NUC1 13C
P1 8.80 usec
P12 2000.00 usec
P26 500.00 usec
PL1 -3.00 dB
PL1W 58.63890457 W
SFO1 100.6233333 MHz
SP2 6.27 dB
SP8 6.27 dB
SPNAM2 Cpd6comp.4
SPNAM8 Cpd6.0.5.20.1
SPOAL2 0.500
SPOAL8 0.500
SPOFFS2 0.00 Hz
SPOFFS8 0.00 Hz
======== CHANNEL f2 ========
CPDPRG2 waltz16
NUC2 1H
PCPD2 90.00 usec
PL2 -4.00 dB
PL12 15.35 dB
PL2W 24.29185867 W
PL12W 0.28213742 W
SFO2 400.1316005 MHz
SI 65536
SF 100.6127690 MHz
WDW EM
SSB 0
LB 2.00 Hz
GB 0
PC 1.00
176.5
134.7
125.1
125.0
82.2
82.1
77.4
77.1
76.8
66.5
66.4
61.4
57.7
51.9
47.9
46.5
46.2
46.1
42.5
41.1
36.7
29.9
29.8
24.1
17.2
16.9
13.3
220 210 200 190 180 170 160 150 140 130 120 110 100 90 80 70 60 50 40 30 20 10 0 ppm

Supplementary Figure S3. (A) ^{1}H NMR spectrum of DMAPT-HCl (d_4-MeOH) and (B) ^{13}C NMR spectrum of DMAPT (d_4-MeOH).

A

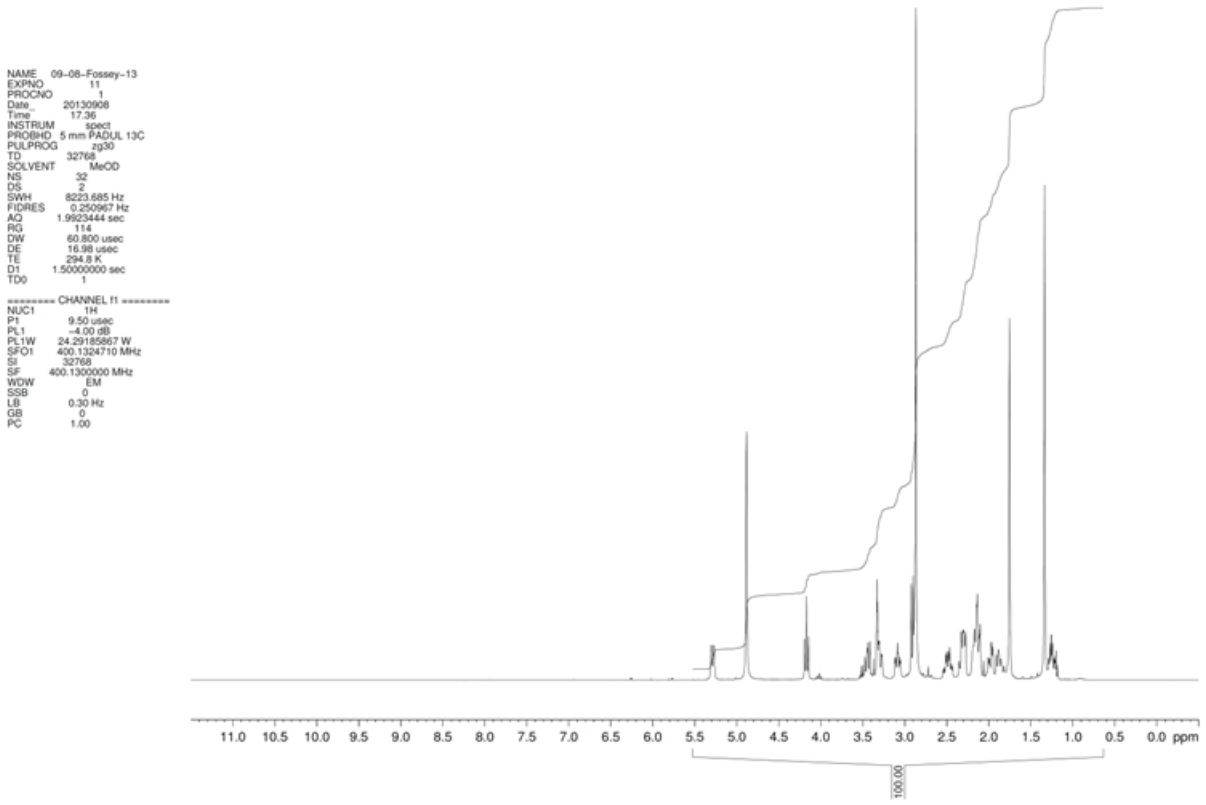

B

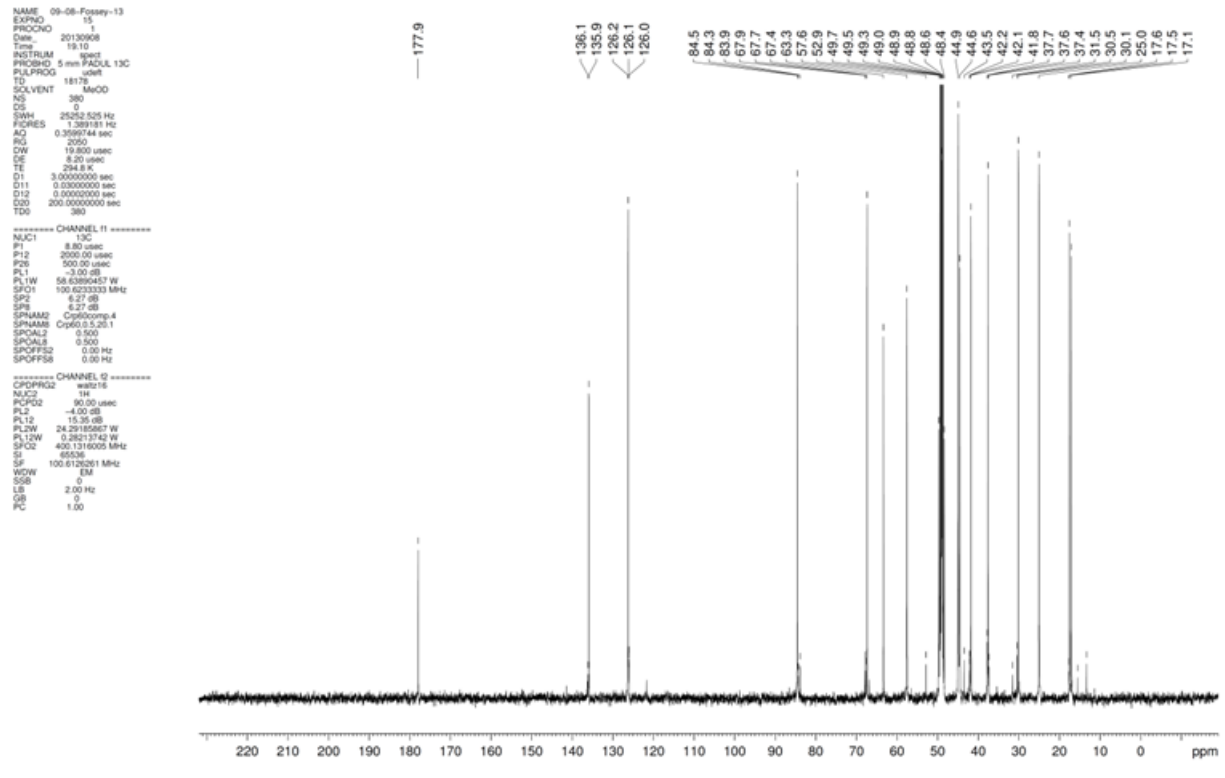

Supplementary Figure S4

(A) Heatmap of previously published microarray data (22) showing the effect of ATM-null status on the expression of 40 NRF2-target genes in response to IR. The data is normalised to the expression values in untreated cells. Each column represents a different patients sample and each row represents a single gene. Colour changes within a row indicate expression levels relative to the average of the same population. Red indicates up-regulation and blue down-regulation. (B) Q-PCR showing defective induction of NRF2-target genes in ATM-wt and ATM-null primary CLLs tumour cells following 6 hours treatment with 10μM tBHQ. (C) Dot plot comparing the ACTIN-normalised Ct values for NRF2 transcripts in ATM-wt and ATM-null primary CLL cells. (D) Immunoblot and (E) densitometric quantification showing comparable induction of NRF2 in whole cell lysates following treatment with tBHQ in a panel of ATM-wt and ATM-null primary CLL tumours. The NRF2 signal was normalised to β-ACTIN. (F) Nuclear [N] and cytoplasmic [C] fractions were generated using primary CLL samples, DMSO treated or treated with 100μM tBHQ for 6 hours. Lysates were separated by SDS-PAGE and immobilised NRF2, KEAP1, BACH1 and MAF1 were visualised using their respective antibodies (Santa Cruz). Antibodies against Lamin B and Tubulin as loading controls. The results show treatment-induced NRF2-nuclear localisation and reduction in the nuclear levels of BACH1. The levels of NRF2, KEAP1, BACH1 and MAF1 are comparable between ATM-wt and ATM-null primary CLL cells. The statistical significance was determined using Student's *t*-test, p-values less than 0.05 (*), 0.001 (***) were considered significant. Error bars represent SEM.

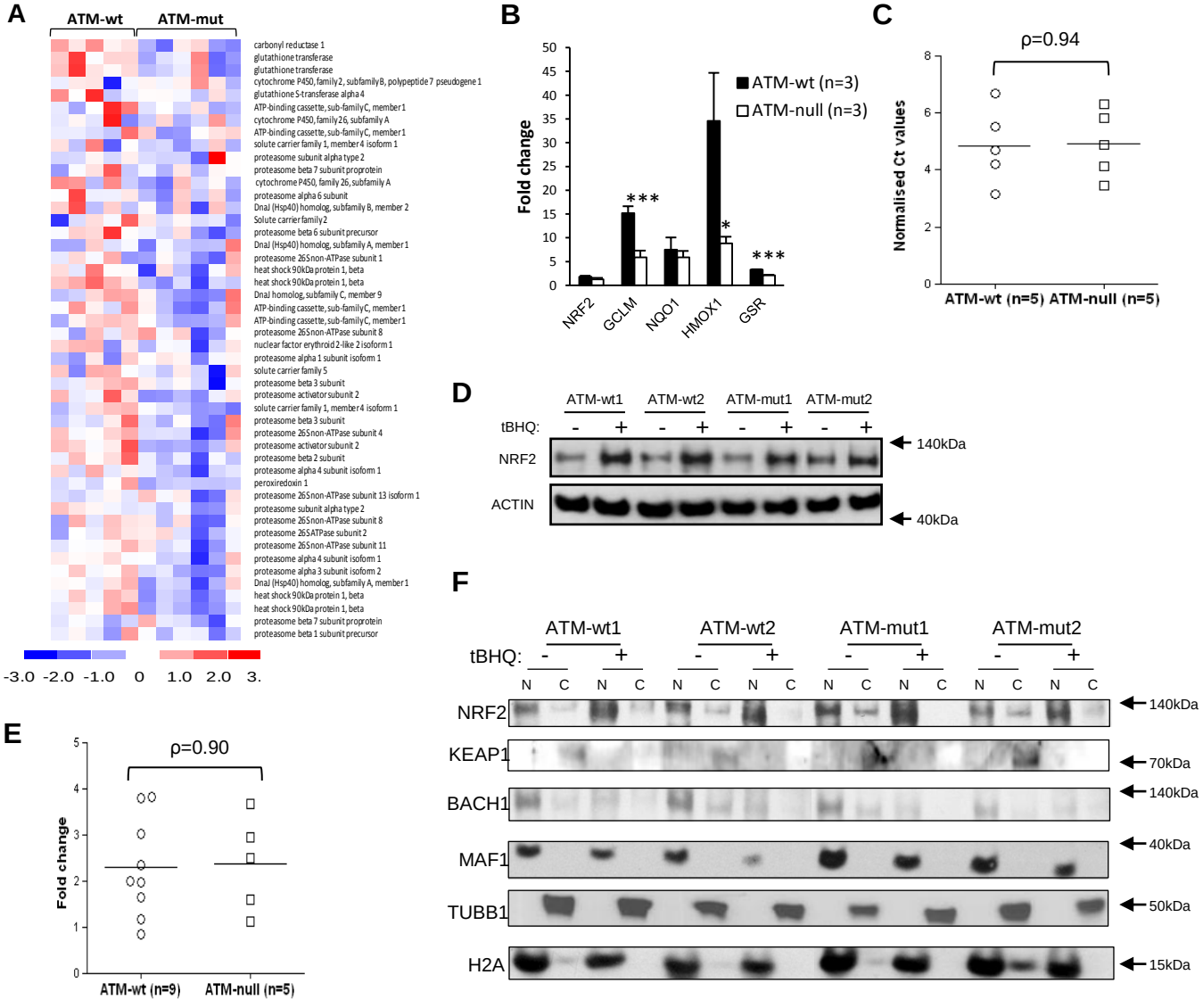

Supplementary Figure S5

A)The interaction between ATM and either NRF2 or PKCδ following treatment with IR , tBHQ or H_2O_2 was investigated in ATM-wt and A-T derived lymphoblastoid cell lines (LCLs) by co-immunoprecipitation. Cells were lysed using NETN buffer (150mM NaCl, 50mM Tris-HCl pH7.8, 1% NP40, protease inhibitor cocktail EDTA-free , 2mM $MgCl_2$ and 90U/ml Benzonase. Pre-cleared lysates containing 6mg of protein were incubated with anti-ATM (cl.11G12, Abcam) or Pre-Immune rabbit IgG (Sigma-Aldrich) and antibody-protein complexes were immobilised on Protein-A sepharose beads, separated by SDS/PAGE and subjected to immunoblotting. Neither NRF2 (rabbit anti-NRF2 (C20), Santa Cruz), or PKCδ co-immunoprecipitated with ATM in ATM-wt or ATM-null LCL cells in response to oxidative stress inducing agents (10Gy IR, 100μM tBHQ, 100μM H_2O_2). **B)** Protein lysates from CII CLL cells treated as indicated were immunoprecipitated with either anti-NRF2 (H300, Santa Cruz) or Pre-Immune IgG. Following immunoblotting of immobilised complexes the effect of ATM inhibition on the level of phospho serine in immunoprecipitated NRF2 was determined. Immunoblots were also probed for NRF2 and small MAFS. Whole cell lysates (WCL) were loaded as imput controls. **C)** Immunoblot showing comparable expression of PKCδ in ATM-wt and ATM-null primary CLLs. Antibody against SMC1 was used as a loading control.

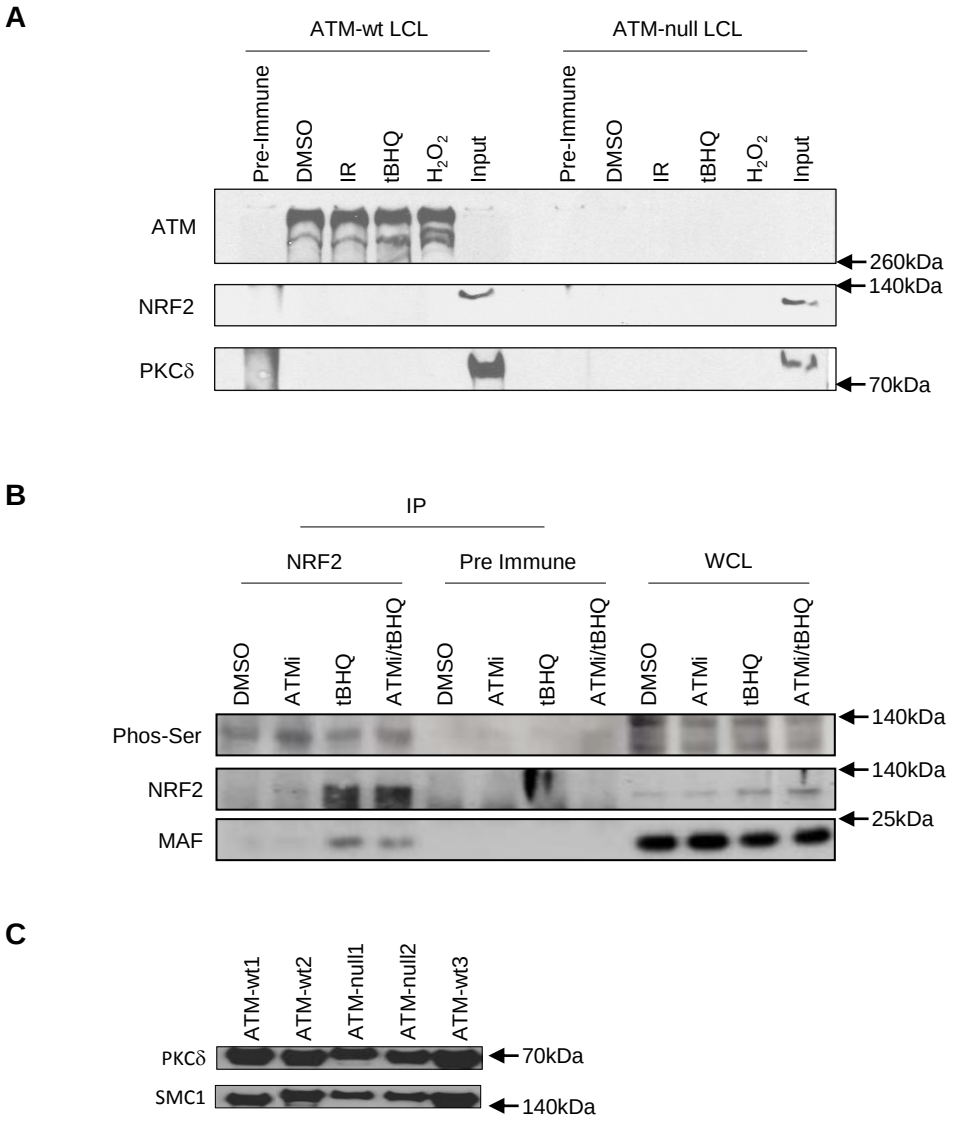

Supplementary Figure S6

(A) Total glutathione levels are reduced in three isogenic CLL cell lines (CII, PGA and HG3) with ATM knock down compared to ATM-wt counterparts. Data is expressed relative to the levels in ATM wild-type cells (GFP shRNA). (B) Q-PCR shows that the mitochondrial DNA content of both ATM-wt and ATM-null primary CLL PBMCs is increased relative to normal donor PBMCs. Mitochondrial DNA was amplified (mtFw-CACCCAAGAACAGGGTTTGT and mtRv- TGGCCATGGGTATGTTGTTAA) and normalised to genomic DNA with primers for 18S rRNA (18SFw-TAGAGGGACAAGTGGCGTTC and 18SRv- CGCTGAGCCAGTCAGTGT) using the comparative Ct method. The statistical significance was determined using Student's *t*-test, p-values less than 0.05 (*), 0.01 (**) were considered significant. Error bars represent SEM.

A

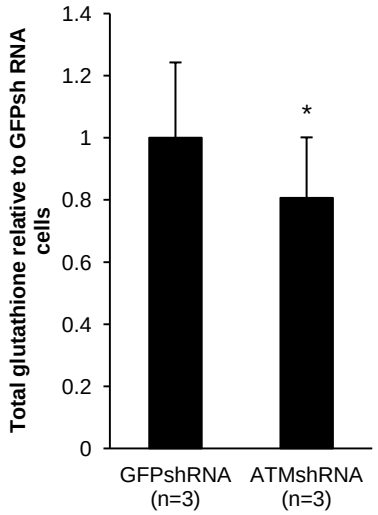

B

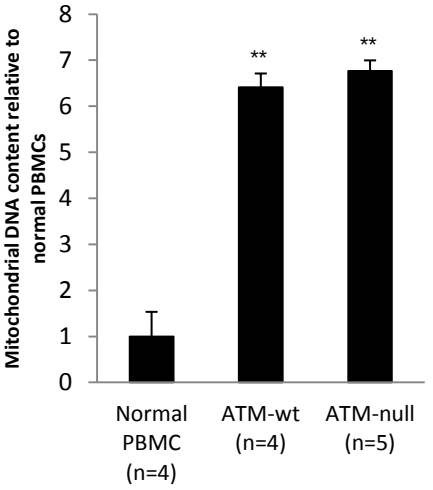

Supplementary Figure S7

CII isogenic cell lines exhibit increased sensitivity to (A) H_2O_2 when ATM is knocked-down. Cells stably expressing the indicated shRNAs were treated with increasing concentrations of H_2O_2 for 24 hours. (B) The sensitivity of ATM-null CLL cells to H_2O_2, (C) NAPQI or (D) parthenolide was diminished by pre-treatment with 20mM NAC. (E) PBMCs (n=2) from normal donors were treated for 24 hours with H_2O_2 or (F) parthenolide. The sensitivity of CLLs with del 11q and TP53 mutations to H_2O_2 (G) and parthenolide (H) was also examined. Surviving fraction was determined by flow cytometry following staining with Annexin V-FITC and propidium iodide. The statistical significance was determined using Student's *t*-test, p-values less than 0.05 (*), 0.01 (**), 0.001 (***) were considered significant. Error bars represent SEM.

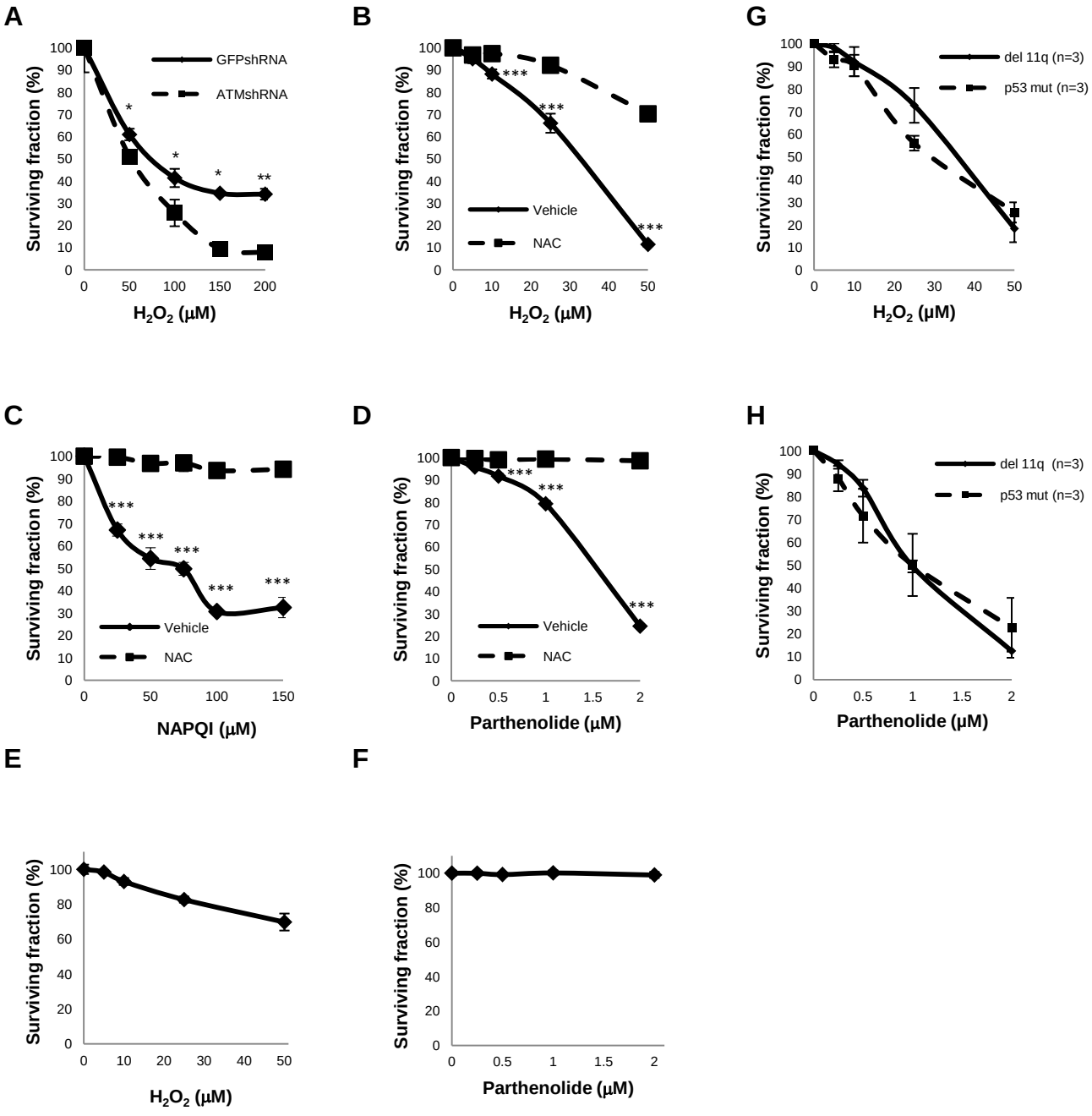

Supplementary Figure S8

Immunoblot showing the effect of H_2O_2 upon phosphorylation of ATM substrates in the DNA damage response (DDR) in representative ATM-wt and ATM-null primary CLL samples. CLL samples were treated for 6 hours with the indicated concentrations of H_2O_2. For the positive control (right, last lane), protein lysate was generated from an ATM-wt sample an hour after treatment with 5 Gy ionising radiation (IR). Data shows that unlike the response to IR, ATM substrates (ATM, SMC1, KAP1 and p53) are not phosphorylated upon exposure to H_2O_2, indicating that DDR is not activated.